# Dalton Transactions

Accepted Manuscript






ROYAL SOCIETY OF CHEMISTRY

www.rsc.org/dalton

Cite this: DOI: 10.1039/c0xx00000x

www.rsc.org/xxxxxx

ARTICLE TYPE

# Probing interactions through space using spin-spin coupling

**Martin W. Stanford,[a] Fergus R. Knight,[a] Kasun S. Athukorala Arachchige,[a] Paula Sanz Camacho,[a] Sharon E. Ashbrook,[a] Michael Bühl,[a] Alexandra M. Z. Slawin[a] and J. Derek Woollins*[a]**

***Received (in XXX, XXX) Xth XXXXXXXXX 20XX, Accepted Xth XXXXXXXXX 20XX***

**DOI: 10.1039/b000000x**

The series of eight 5-(TeY)-6-(SePh)acenaphthenes (Y = Fp (**2**), Tol (**3**), An-*p* (**4**), An-*o* (**5**), Tp (**6**), Mes (**7**), Tip (**8**), Nap (**9**)) were prepared and structurally characterised by X-ray crystallography, solution and solid-state NMR spectroscopy and density functional theory (DFT/B3LYP) calculations. All members of the series, except **5**, adopt a BA type configuration comparable to the parent compound **1** (Y = Ph), aligning the Te-$C_Y$ bond along the mean acenaphthene plane and promoting a nonbonded Se···Te-$C_Y$ 3c-4e type interaction to form to stabilise the molecule (G-dependence). **5** (Y = An-*o*) adopts a BC type conformation in the solid but DFT calculations show this optimises to BA. Indication of strong through-space *peri*-interactions between Te and Se are observed in the $^{77}$Se and $^{125}$Te NMR spectra, with $^{1}J$(Te,Se) spin-spin coupling constants (SSCCs) in the range -688 to -748 Hz. Evidence supporting the presence of this interaction was also found in solid-state NMR spectra of some of the compounds which exhibit an indirect spin-spin coupling on the same order of magnitude as observed in solution. In order to quantify the steric bulk of the aryl groups (Y), we introduce the crystallographic steric parameter (θ), the cone angle measured from the furthest H atoms lying on the edges of the cone to the Te atom located at its vertex. Modification to Y has no apparent influence over the conformation of the molecule, the degree of molecular distortion occurring in the acenaphthene backbone or the extent of 3c-4e interaction; *peri*-distances for all eight compounds are within 0.08 Å and no apparent correlation is observed between the steric bulk of Y (θ) and the $^{77}$Se chemical shifts or $^{1}J$(Te,Se) SSCCs. In contrast, a good correlation is found between θ and $^{125}$Te chemical shifts. DFT calculations performed on all members of the series confirm the comparable covalent bonding between Te and Se in the series, with WBIs of *ca*. 0.1 obtained. Natural bond orbital analysis shows a noticeable donor-acceptor interaction between a p-type lone pair on Se and a σ*(Te-C) antibonding orbital, confirming the onset of 3c-4e type bonding.

## Introduction

The magnitude of NMR spin-spin coupling constants (SSCCs) is dependent upon the interaction between the magnetic moments of the coupling nuclei and can provide important information for analysing molecular structures.[1-3] Indirect (scalar) coupling is transmitted by polarisation of the electrons in the succession of bonds connecting the nuclei (through-bond coupling) and generally diminishes as the number of bonds between the two nuclei increases, with coupling beyond four bonds usually too small to be observed.[1-3]

Nevertheless, remarkably large coupling constants have been detected in molecules in which NMR active atomic nuclei lie many bonds apart but are located in close proximity (formally nonbonded), with spin-spin coupling transmitted through the interaction of overlapping lone pairs (through-space coupling).[3-8] Such spatial proximity can be achieved across the bay region in *peri*-substituted naphthalenes and related 1,2-dihydro-acenaphthylenes (acenaphthenes), where large heteroatoms, fixed by the rigid organic framework, have typical separations of around 3 Å.[9] For instance, surprisingly large $^{1}J$($^{19}$F,$^{19}$F) SSCCs, long known to exist between intramolecularly confined fluorine atoms, have been observed in *peri*-difluoronaphthalenes (**A** & **B** Figure 1; 65-85 Hz), the magnitude attributed to a significant $^{19}$F-$^{19}$F through-space coupling component and directly dependent upon the internuclear F···F distance.[5,6] Exceptionally large $^{4}J$($^{31}$P,$^{31}$P) coupling constants have similarly been observed in 1,8-diphosphanaphthalenes (**C** Figure 1) which also represent systems possessing lone pairs available for interaction through space.[7,10,11] In fact the values reported for Nap[P(NMe$_2$)$_2$][P(OMe)(NMe$_2$)] (246 Hz),[10] Nap(PH$_2$)$_2$ (222 Hz)[7] and Nap(PPh$_2$)$_2$ (199 Hz; obtained from MAS solid state $^{31}$P{$^{1}$H} NMR spectrum)[11] are more in line with $^{1}J$-couplings found in systems with conventional P-P bonds (180-230 Hz).[10] $^{1}J$($^{77}$Se,$^{77}$Se) nuclear couplings have also been investigated in detail through quantum chemical (QC) calculations[8] in order to investigate the nature of bonded and nonbonded interactions between Se atoms in *peri*-substituted naphthalenes. Notably large $^{4}J$-couplings were observed in Se···Se (332 Hz), Se···Se=O (189-200 Hz) and O=Se···Se=O (456 Hz) derivatives (**D** & **E** Figure 1), with the latter the largest known value for $^{4}J$-coupling between two formally nonbonded Se atoms.[8]

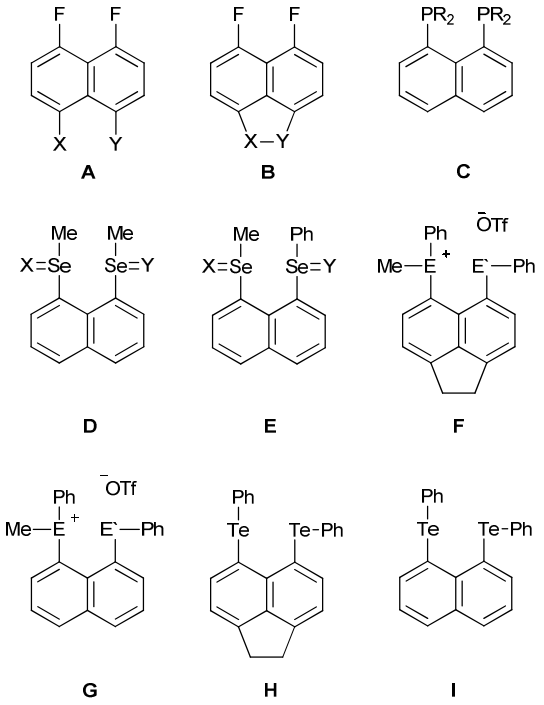


**Fig. 1** Naphthalene and acenaphthene motifs allowing for the overlap of lone-pair orbitals leading to through-space coupling interactions.

Considering spin polarisation and therefore the value of the through-space coupling is dependent upon the spatial distribution of electron density between the coupling nuclei, SSCCs provide a convenient method of analysing the electronic structure of a system and can indicate the onset of intramolecular bonding interactions. For many years we have been investigating non-covalent interactions which prevail when pnictogen and chalcogen congeners are located at the *peri*-positions of naphthalene and acenaphthene.[12-21] Under appropriate geometric conditions, weak donor-acceptor interactions can transpire leading to 3c-4e type bonding, which becomes more prevalent as larger atoms occupy the proximal positions.[13-18,20] In all cases, *peri*-separations are well within the sum of van der Waals radii for the two substituted heteroatoms and Wiberg bond indices[22] of up to ca. 0.15 have been computed for bis-tellurium derivatives (**F** & **G** Figure 1).[17] Direct observation of strong through-space *peri*-interaction is detected in the $^{77}$Se and $^{125}$Te NMR spectra of unsymmetrical Acenap(TePh)(SePh) (**1**, Figure 2) and its naphthalene analogue, which display exceptionally large, formally $^{4}J$, SSCCs of -716 Hz and -834 Hz, respectively.[17,18] Even larger WBIs up to 0.18 are obtained for the cationic salts formed by methylation of the neutral chalcogen substituted compounds (**H** & **I** Figure 1), and these too exhibit considerable through-space coupling [$J$($^{77}$Se,$^{77}$Se) **H** 141, **I** 167 Hz; $J$($^{125}$Te,$^{77}$Se) **H** 382, **I** 429 Hz; $J$($^{125}$Te,$^{125}$Te) **H** 946, **I** 1093 Hz].[18,23]

We have recently reported even greater SSCCs in symmetrical bis-tellurium systems Acenap(TePh)$_2$ (2110 Hz) and Nap(TePh)$_2$ (2505 Hz),[24] in which weak donor-acceptor interactions, marking the onset of 3c-4e bonding, greatly enhance the Te,Te couplings and thus contribute to the magnitude of the $J$($^{125}$Te,$^{125}$Te) values.[20] The large discrimination between the $J$ values in these two analogues, however, suggests the effective overlap of the tellurium lone-pairs and hence the size of the SSCCs, depends not only on the intramolecular Te···Te *peri*-distance, but also on the orientation of the lone-pairs, similar to reported angular dependence found in FF and SeSe systems.[5,8] Detailed conformational analyses carried out on the related bis-tellurium compound Nap(TeMe)$_2$[20] and bis-selenium derivatives[8] have shown that a minor change in conformation can result in a dramatic change in the magnitude of SSCCs, for example a structure with CC*t* conformation (*vide infra*)[25,26] would have a $J$ value of around 2500 Hz, similar to what is found for Nap(TePh)$_2$, whilst a structure in the AB region, as adopted by Acenap(TePh)$_2$,[17] would be much lower (ca. 1500 Hz).[20] This characteristic of SSCCs to act as a sensitive probe for distinguishing between differing conformers of a molecule is a new facet of through-space spin-spin coupling, and one worth further investigation. In the present study, we explore how substituents at the phenyl ring affect the bonding interactions and hence the value of SSCCs in a series of mixed Te,Se acenaphthenes Acenap(TeY)(SePh) (Y = Fp **2**; Tol **3**; An-*p* **4**; An-*o* **5**; Tp **6**; Mes **7**; Tip **8**; Nap **9**; Figure 2) compared with the parent phenyl substituted compound **1**.[17]

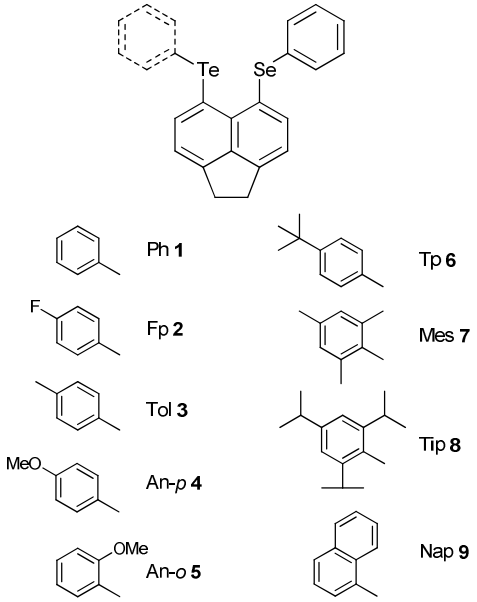


**Fig. 2** 5-(aryltelluro)-6-(phenylselenyl)acenaphthenes **1-9**

## Results and Discussion

**Synthesis of 5-(aryltelluro)-6-(phenylselenyl)acenaphthenes 2-9:** The eight mixed tellurium-selenium substituted acenaphthenes **2-9** were prepared following the same procedure to that previously reported for the synthesis of 5-(phenyltelluro)-6-(phenylselenyl)acenaphthene **1**;[17] under an oxygen- and a moisture-free nitrogen atmosphere, 5-bromo-6-(phenylselenyl)acenaphthene was independently treated with a single equivalent of *n*-butyllithium in diethyl ether to afford the precursor 5-(lithio)-6-(phenylselanyl)acenaphthene, which when reacted with the respective diaryl ditelluride [bis(4-fluorophenyl) ditelluride (FpTeTeFp), bis(4-methylphenyl) ditelluride (TolTeTeTol), bis(4-methoxyphenyl) ditelluride (An-*p*TeTeAn-*p*), bis(2-methoxyphenyl) ditelluride (An-*o*TeTeAn-*o*), bis(4-

Cite this: DOI: 10.1039/c0xx00000x

www.rsc.org/xxxxxx

# ARTICLE TYPE

**Table 1** $^{77}$Se and $^{125}$Te NMR spectroscopy data and the crystallographic steric parameter (θ)

| | **1**[17] | **2** | **3** | **4** | **5** | **6** | **7** | **8** | **9** |
|---|---|---|---|---|---|---|---|---|---|
| **Aryl Group** | **Ph** | **Fp** | **Tol** | **An-*p*** | **An-*o*** | **Tp** | **Mes** | **Tip** | **Nap** |
| **$^{77}$Se NMR** | 341 | 340 | 342 | 342 | 347 | 343 | 345 | 345 | 400 |
| **$^{125}$Te NMR** | 663 | 653 | 649 | 639 | 544 | 643 | 428 | 376 | 552 |
| ***J*($^{125}$Te-$^{77}$Se)** | -716 | -726 | -723 | -722 | -748 | -723 | -711 | -688 | -724 |
| ***J*($^{125}$Te-$^{77}$Se) (comp.)**[b] | -526[c] | -484 | -471 | -537 | -585 | -468 | -519 | -469 | -460 |
| **θ** | 81.22 | 80.98 | 80.43 | 81.02 | 103.34 | 80.46 | 121.55 | 134.98 | 102.84 |

[a] All spectra run in $CDCl_3$; δ (ppm), *J* (Hz), θ (°); [b] Computed at the ZORA-SO/BP86/TZ2P level; [c]ZORA-SO/PBE0 level: *J* = -571 Hz.

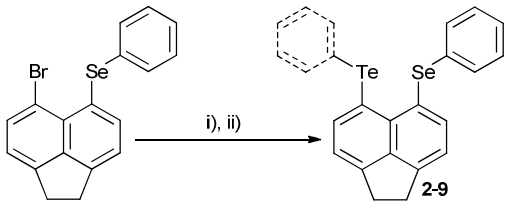


**Scheme 1** The preparation of 5-(aryltelluro)-6-(phenylselenyl)acenaphthenes **2-9**: (i) *n*BuLi (1 equiv), $Et_2O$, −78 °C, 1 h; (ii) ArylTeTeAryl (1 equiv), $Et_2O$, −78 °C, 1 h (Aryl: Ph **1**; Fp **2**; Tol **3**; An-*p* **4**; An-*o* **5**; Tp **6**; Mes **7**; Tip **8**; Nap **9**).

*tert*butylphenyl) ditelluride (TpTeTeTp), bis(2,4,6-trimethylphenyl) ditelluride (MesTeTeMes), bis(2,4,6-triisopropanylphenyl) ditelluride (TipTeTeTip) and bis(1-naphthyl) ditelluride (NapTeTeNap)] afforded **2**–**9** in moderate to good yield [yield: 43 (**2**), 42 (**3**), 69 (**4**), 67 (**5**), 23 (**6**), 18 (**7**), 56 (**8**), 86% (**9**); Scheme 1]. All compounds obtained (**2**–**9**) were characterized by multinuclear magnetic resonance and IR spectroscopies and mass spectrometry, and the homogeneity of the new compounds was confirmed by microanalysis. Solution- and solid-state $^{77}$Se and $^{125}$Te NMR spectroscopic data for the series of acenaphthene derivatives is displayed in Table 1.

**Solution- and Solid-State NMR Studies:** As expected, the $^{77}$Se NMR and $^{125}$Te NMR spectra for all nine compounds exhibit single peaks, with satellites attributed to $^{125}$Te-$^{77}$Se coupling. The relatively large *J* values (-687 Hz (**8**) to -749 Hz (**5**)) indicate a potential weakly attractive through-space interaction between Te and Se in each case, however, the range of values lie within 62 Hz and there is no discernible correlation with the steric bulk of the Te(aryl) moiety. The negative sign attributed to the experimental *J* values is taken from the computed *J* values for the Te,Se systems and stems from the opposite signs of the gyromagnetic ratios of $^{77}$Se (5.12 x $10^7$ rad $T^{-1}$ $s^{-1}$) and $^{125}$Te (-8.51 x $10^7$ rad $T^{-1}$ $s^{-1}$).[2]

Compared to experiment, the computed[27] *J*($^{125}$Te,$^{77}$Se) SSCCs are significantly underestimated (-460 Hz to -585 Hz). The theoretical *J* values are mildly dependent on the functional employed in the NMR calculation, becoming slightly more negative on going from BP86 to PBE0 (e.g. by -45 Hz for **1**, Table 1). Theory and experiment agree that the *J*($^{125}$Te,$^{77}$Se) couplings should be much smaller than the corresponding ($^{125}$Te,$^{125}$Te) couplings in ditelluride derivatives. At the same level (BP86), a *J*($^{125}$Te,$^{125}$Te) value of 1543 Hz was predicted for Acenap(TePh)$_2$, with *J*($^{123}$Te,$^{125}$Te) 1750 Hz detected as satellites in the $^{123}$Te NMR spectrum, corresponding to 2110 Hz in *J*($^{125}$Te,$^{125}$Te).[20] The computed reduced coupling constant (K) gives a more direct comparison of couplings involving different sets of nuclei.[28] Upon moving down one row in the periodic table K increases significantly, nearly doubling from $K = 720 \cdot 10^{19}$ kg $m^{-2}$ $s^{-2}$ $A^{-2}$ in Acenap(TePh)(SePh) to $K = 1273 \cdot 10^{19}$ kg $m^{-2}$ $s^{-2}$ $A^{-2}$ in Acenap(TePh)$_2$ (computed for BA conformers).[20] The Fermi contact mechanism, whereby two coupling nuclei are in contact via the s-electrons of the bonds linking them, is widely considered the dominant factor in spin-spin coupling[2] and has been confirmed to govern the (Te,Te) coupling constants in Acenap(TePh)$_2$.[20] The same is found for compounds **1** - **9** of this study, where diamagnetic spin-orbit contributions are negligible and paramagnetic spin-orbit contributions are less than 14 Hz at the ZORA-SO level. The magnitude of the coupling constant is thus influenced by the extent of s-orbital participation in the bonding and the polarisability of the s-electrons, which is controlled by the spin of the respective nuclei involved.[2] The natural increase in the polarisability of valence s-electrons down the periodic table thus explains the dramatic difference observed between (Te,Se) and (Te,Te) coupling constants (and similarly for the reduced coupling constants, K), with significantly reduced *J* values expected between lighter congeners.

A further consideration for molecules in which heteroatoms are held in close proximity, but formally non-bonded, is the degree to which the observed coupling results from a direct overlap of lone pair orbitals (through-space coupling). The structural configuration of the molecule thus influences the degree to which electron density is delocalized over the formally nonbonded atoms, and hence the contribution to the bonding occurring between these atoms.[5,8,20] The propensity for compounds **1**-**9** to adopt the BA configuration[25,26] is thus partly responsible for the smaller *J*(Te,Se) couplings compared to *J*(Te,Te), whilst further reduction is likely due to the decreased multicenter bonding compared to the bis-tellurium systems (*vide infra*).

The small range of $^{77}$Se NMR chemical shifts for **1**-**8** (~8 ppm) reveals the chemical similarity of the Se nuclei throughout the series and suggests the change in size of the Te(aryl) group has a limited effect on the chemical shielding of the Se nucleus. The

Cite this: DOI: 10.1039/c0xx00000x

www.rsc.org/xxxxxx

# ARTICLE TYPE

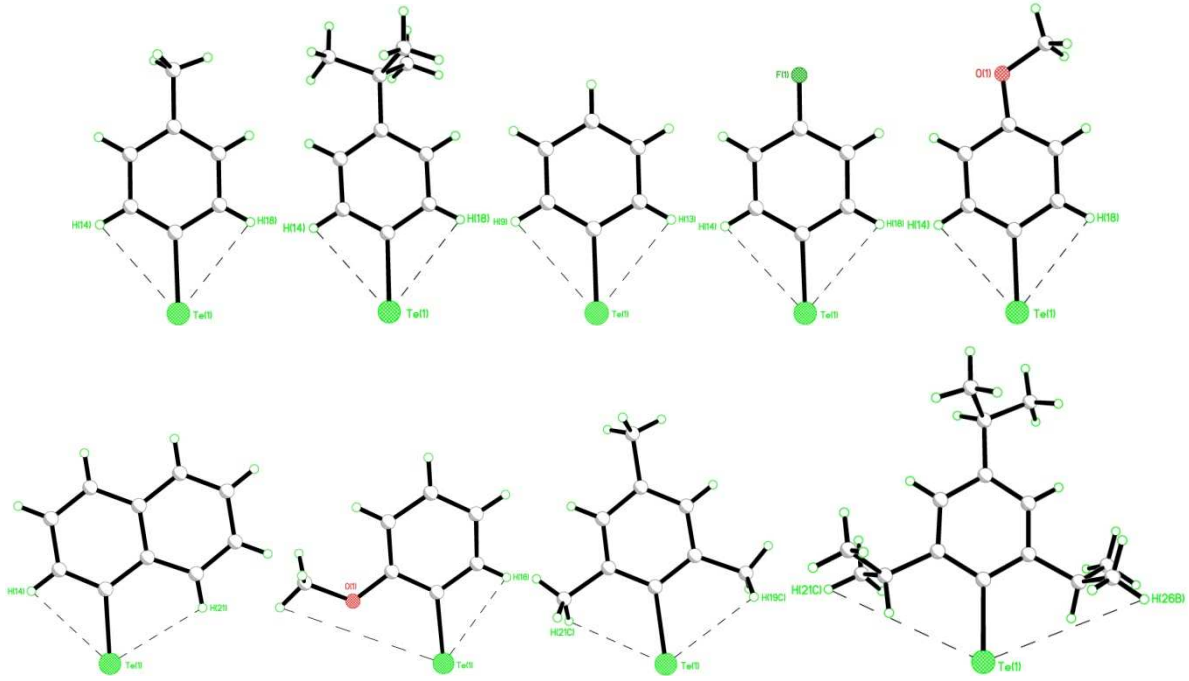

**Fig. 3** The Te(aryl) moieties of **1-9** illustrating the crystallographic steric parameter θ defined by the largest measurable H-Te-H cone angle.

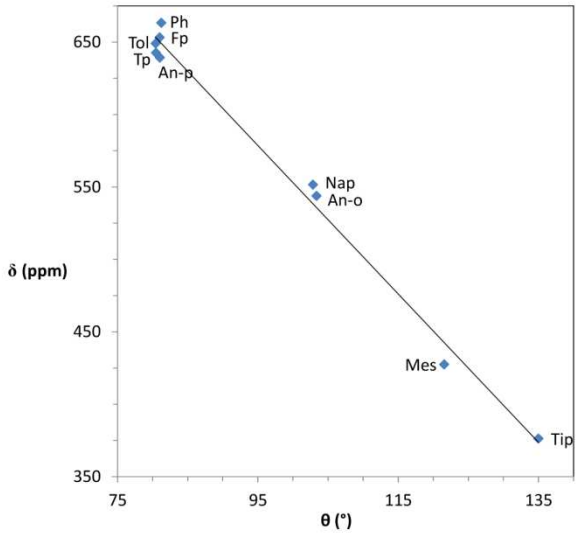


**Fig. 4** Plot of $^{125}$Te NMR chemical shifts against the crystallographic steric parameter θ using data from Table 1 for compounds **1-9.**

one exception in the series is compound **9** (TeNap) which displays a notable downfield shift to 399.9 ppm, compared with the remaining members of the series (340-347 ppm). In contrast, modification of the size and electronics of the aryl moiety has a greater influence on the $^{125}$Te NMR signals, which are generally shifted upfield (to lower chemical shift) as less encumbered groups on Te are replaced by much bulkier ones (**1** phenyl 663.4 ppm; **8** triisopropylphenyl (Tip) 376.4ppm).

In order to correlate the $^{125}$Te NMR chemical shifts with the steric bulk of the aryl functionalities, Te(aryl) group cone angles have been calculated from crystallographic data to provide a quantitative measure of the steric bulk. The steric parameter (θ), which is a slight modification of the Tolman Cone Angle,[29] is defined by the apex angle measured from the hydrogen atoms occupying the extreme edges of a cone to the centre of the Te atom located at its vertex. Figure 3 illustrates the increasing steric bulk for the Te(aryl) groups in compounds **1-9** as defined by the magnitude of the steric parameter (θ).

$^{125}$Te NMR data for **1-9** plotted against θ show a good correlation between chemical shift magnitude and the size of the Te(aryl) group (Figure 4). The large range of tellurium chemical shifts in the present series can therefore be explained in terms of steric crowding, despite the apparent similarity of the aryl group electronegativities. A similar observation has previously been observed in tertiary phosphines, with a good correlation between the Tolman cone angle and $^{31}$P NMR shifts.[29]

$^{77}$Se and $^{125}$Te solid-state NMR spectra were recorded for compounds **6** and **8**, and the splittings observed for both compounds confirm the presence of a weak interaction between Se and Te. However, the presence of a significant chemical shift anisotropy (CSA) in both cases results in a number of spinning sidebands, hindering the accurate analysis of both shielding and coupling tensors. The splittings observed in the isotropic peak are between 640 and 700 Hz in both cases, although a more detailed analysis would be required to extract the full information on both interactions. As an example the $^{77}$Se and $^{125}$Te spectra of

compound **8** are shown in Figures 5 and 6.

Crystal structures of compounds **8** and **6** contain one crystallographically distinct molecule per asymmetric unit, however, two isotropic peaks were found for both samples due to maybe the presence of some impurities present in the bulk material.

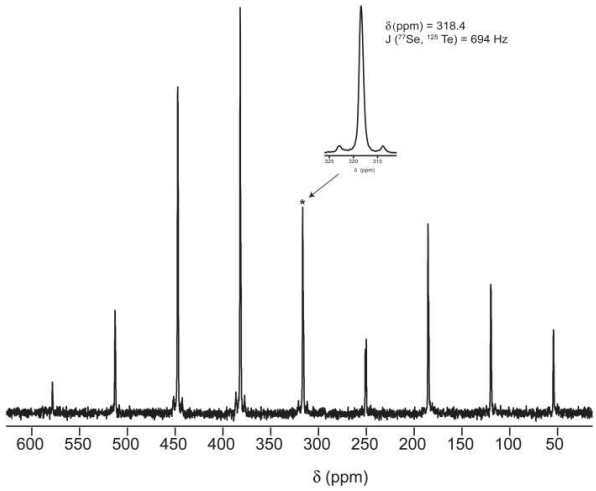


**Fig. 5** $^{77}$Se solid-state (B0 = 9.4 T) NMR spectra of compound **8**, recorded using an MAS rate of 5 kHz for the full spectrum and 40 kHz for the expanded view of the isotropic peak (indicated by *). The values quoted correspond to the isotropic chemical shift and the splitting observed in the isotropic peak.

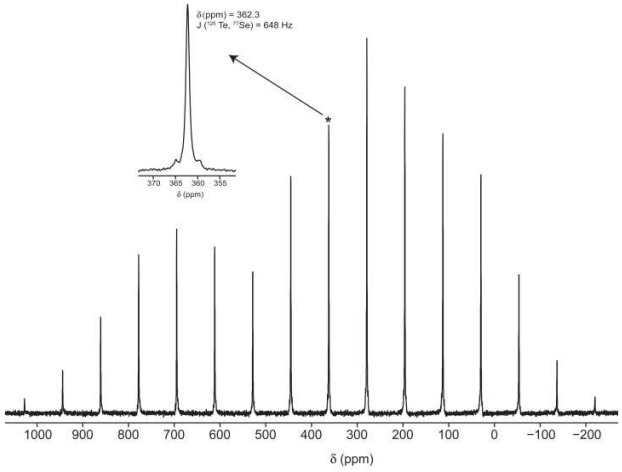


**Fig. 6** $^{125}$Te solid-state (B0 = 9.4 T) NMR spectra of compound **8**, recorded using an MAS rates of 10.5 kHz. The values quoted correspond to the isotropic chemical shift and the splitting observed in the isotropic peak (also shown expanded).

### X-ray investigations

Suitable single crystals were obtained for **2-9** by diffusion of hexane into a saturated solution of the compound in dichloromethane. Compounds **3** and **5** crystallise with virtually identical molecules in the asymmetric unit, in contrast to the remaining members of the series which contain one molecule in the asymmetric unit. Selected interatomic bond lengths and angles and computational properties are listed in Tables 2-6. Further crystallographic information can be found in the Supporting Information.

Molecular structures of *peri*-substituted systems are conveniently classified by three types A, B and C, describing the conformation of the E-$C_{Ar}$ bond with respect to the mean naphthalene plane as either perpendicular (**A**), along the plane (**B**) or intermediate between these two scenarios (**C**). A double substitution of aryl functionalities can subsequently align either *cis* (*c*) or *trans* (*t*) relative to the naphthalene plane.[17,25] The labels planar (**pl**), perpendicular (**pd**) and non-planar/non-perpendicular (**np**) are additionally employed to describe the conformation around the E-$C_{Ar}$ bond.[25] The absolute conformation of aromatic rings is calculated from torsion angles θ and γ, which define the degree of rotation around the E-$C_{Acenap}$ (**A**, **B**, **C**) and E-$C_{Ar}$ (**pl**, **pd**, **np**) bonds, respectively (Table 6, Figure S2, ESI).[17,25,26]

The energy lowering effect of the (G)···σ*(E-$C_{Ar}$) 3c-4e interaction has been shown to play an important role in controlling the fine structures of *peri*-substituted systems (G-dependence),[13-18,20,25] although the sterics and electronics of the aryl groups attached to the *peri*-atoms must also be considered (Y-dependence).[25] Minor adjustments to the size and donor/acceptor properties of Y can have a dramatic affect on the structural conformation, forcing substituents to change between the extremes of a type A or B configuration.[25]

As mentioned above, compounds **2-9** prefer to adopt BA type configurations, illustrating the similar Y-dependence of the aryl groups involved, despite the notable change in steric bulk within the series (Table 6, Figure 7). In each case the Te-$C_{Ar}$ bond aligns along the acenaphthene plane (type **B**) and provides the correct geometry to promote delocalization of a selenium lone pair (G) to the antibonding σ* (Te−C) orbital, thus forming a weakly attractive 3c-4e type interaction (G-dependence). Se···Te-$C_{Ar}$ angles are in the range 162-173° and nonbonded *peri*-distances are ~18% shorter than the sum of van der Waals radii for Te and Se (3.96 Å).[30] The elongation and weakening of the Te-$C_{Ar}$ bonds (2.11-2.16 Å) also provides support for the formation of hypervalent 3c-4e bonding interactions across the *peri*-gap. This is observed at the B3LYP level, where the Te-$C_{Ph}$ bond length increases from 2.131 Å in Acenap(TePh) (with the same conformation of the Ph group as in **1**) to 2.154 A in **1**. In addition, Te-$C_{Ar}$ WBIs decrease noticeably in the sequence, from 0.94 to 0.86, which is also consistent with the weakening of the Te-C(aryl) bond expected from the lp(Se)···σ*(Te-$C_{Ar}$) orbital interaction.

In general, the plane of the Te(aryl) group aligns perpendicular (**pd**) to the mean acenaphthene plane, although the Te(nap) group in **9** twists around the Te-$C_{Nap}$ bond aligning the naphthalene plane neither perpendicular or coplanar (**np**) with the acenaphthene backbone. Compound **5** (Te-An-*o*) is the one anomaly in the series, adopting a BC type configuration in which the Se(Ph) moiety aligns with a twist geometry (**C**) with respect to the acenaphthene plane (Figure 8, Table 6). Computational conformational analysis, however, has shown that dramatically different conformations can have similar potential energies (within ~1 kcal mol$^{-1}$),[20] thus consistent with the structural variation found in the solid for compound **5** (see also below). In addition, density functional theory (DFT) calculations show that all members of the series, including **5**, optimise to a BA conformation at the B3LYP/SDD/962(d)/6-31G(d) level. Throughout the series, the plane of the Se(Ph) moiety generally aligns coplanar (**pl**) with the acenaphthene ring, although **pd** and

Cite this: DOI: 10.1039/c0xx00000x

www.rsc.org/xxxxxx

# ARTICLE TYPE

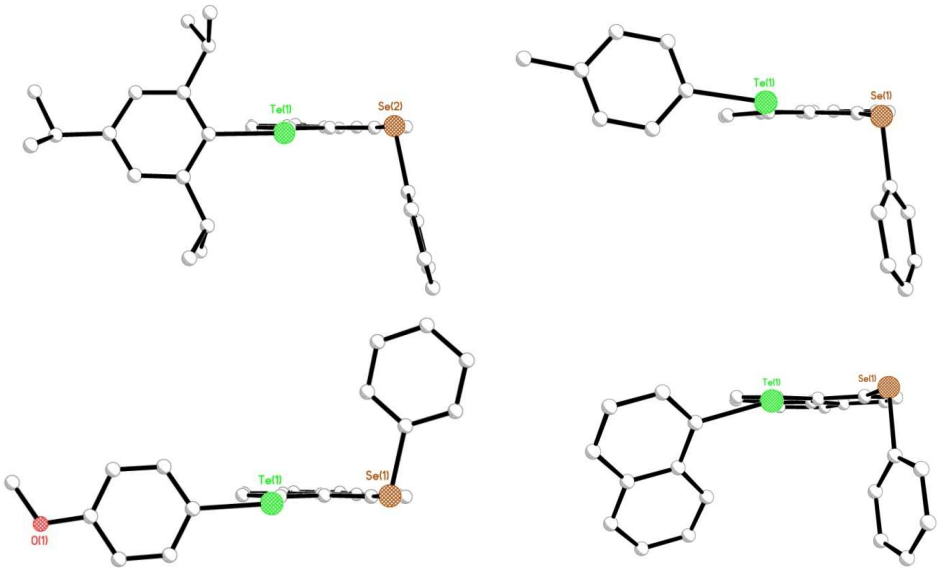


**Fig. 7** The majority of compounds in this study adopt the BA type configuration, with minor differences between the structures resulting from rotation around the E-$C_{Ar}$ bonds: clockwise from top left: Te(Tip) **8** (**B**:**pd**; **A**:**pl**), Te(Tol) **3** (**B**:**pd**; **A**:**np**), Te(Nap) **9** (**B**:**np**; **A**:**pl**), Te(An-p) **4** (**B**:**pd**; **A**:**pd**); H atoms omitted for clarity. The structures of **2**, **6** and **7**, adopting the same structural conformation as **8**, are omitted here put can be found in the ESI.

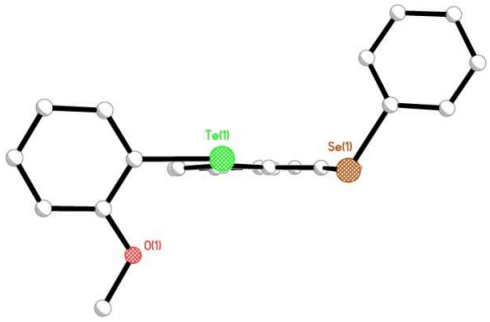


**Fig. 8** Te(An-o) **5** adopts an anomalous structure to the remaining members of the series, the Se(Ph) moiety aligning with a twist (**C**) orientation (**B**:**pd**; **C**:**np**); H atoms omitted for clarity.

**np** variations are observed for compounds **3**-**5**.

The similarity of the structural configurations adopted by compounds **1**-**9** implies the steric bulk of the Te(aryl) moiety plays little part in determining the overall geometry of the molecule. This lack of dependence upon the form of the Te(aryl) group is mirrored in the architecture of the acenaphthene fragment of each compound, with no apparent correlation between the steric bulk of the Te(aryl) functionality and thedegree of molecular distortion occurring within the organic framework. This is best highlighted by comparing the nonbonded Te···Se *peri*-distances which are all within 0.08 Å, spanning a range from 3.2098(6) Å in **8** Te(Tip) to 3.2809(7) Å in **7** Te(Mes). In plane distortion, measuring the divergence of the exocyclic E-$C_{Ar}$ bonds within the acenaphthene plane, varies inconsistently throughout the series with splay angles (sum of the bay region angles – 360°) ranging from 15.4°-18.7°.

Interestingly, compounds substituted by the larger aryl moieties (**8** Tip, **7** Mes, **9** Nap, **5** An-*o*, **4** An-*p*) display the greatest degree of planarity, experiencing only minor deformation of the organic framework (central C-C-C-C acenaphthene torsion angles 0.1-2.5°) and with *peri*-atoms displaced to a maximum 0.3 Å from the mean plane. The remaining members of the series (**1** Ph, **2** Fp, **3** Tol, **6** Tp) display greater deformation, with minor buckling of the organic backbone (central torsion angles 1-4°) combined with greater out-of-plane distortion (displacement from the plane 0.3-0.4 Å).

### DFT Calculations

In order to assess the extent of three-centre, four-electron type interactions occurring in the series, density functional theory (DFT/B3LYP) calculations were performed for the whole set of compounds of this study.[27] All nine structures optimised to a BA conformation with essentially perpendicular and in-plane alignment of the SePh and TeY moieties, respectively. In all cases, except for **5**, the most stable conformer corresponded to the solid state structure. For **5**, the energy span between the optimised BA form and the observed BC variant is remarkably small. Freezing all non-hydrogens and only optimising the H-positions results in the BC structure lying 3.2 kcal $mol^{-1}$ above the fully optimised minimum, however, relaxing all parameters except the two torsion angles C10-C1-Te1-$C_Y$ and C10-C9-Se1-$C_{Ph}$ (Table 3), affords a structure only 0.6 kcal $mol^{-1}$ above the minimum. It thus costs precious little to move between conformations by rotation of the E(aryl) moieties, as previously observed in the Nap($TeMe_2$) model.[20]

From structural analyses (*peri*-distances within 0.08 Å) and comparable SSCCs obtained in the $^{77}Se$ and $^{125}Te$ NMR spectra

Cite this: DOI: 10.1039/c0xx00000x

www.rsc.org/xxxxxx

# ARTICLE TYPE

**Table 2** Computed properties of Acenap(TeAr)(SePh) derivatives (B3LYP level)

| | 1 Ph | 2 Fp | 3 Tol | 4 An-P | 5 An-o | 6 Tp | 7 Mes | 8 Tip | 9 Nap |
|---|---|---|---|---|---|---|---|---|---|
| d(Te···Se) Å | 3.273[a] | 3.274 | 3.282 | 3.282 | 3.273 | 3.285 | 3.287 | 3.292 | 3.279 |
| *X-ray* | *3.248* | *3.218* | *3.229/3.202* | *3.213* | *3.279/3.213* | *3.233* | *3.281* | *3.210* | *3.233* |
| WBI | 0.11 | 0.11 | 0.11 | 0.11 | 0.11 | 0.11 | 0.11 | 0.10 | 0.11 |

[a] PBE0 level: 3.220 Å (WBI 0.12).

**Table 3** Computed and measured torsion angles for BA and BC conformers of **5**

| Level | C10-C1-Te1-C13 | C10-C9-Se1-C20 | Conformation |
|---|---|---|---|
| X-ray | -179.8 | -122.4 | **BC** |
| B3LYP | -168.6 | -100.9 | **BA** |

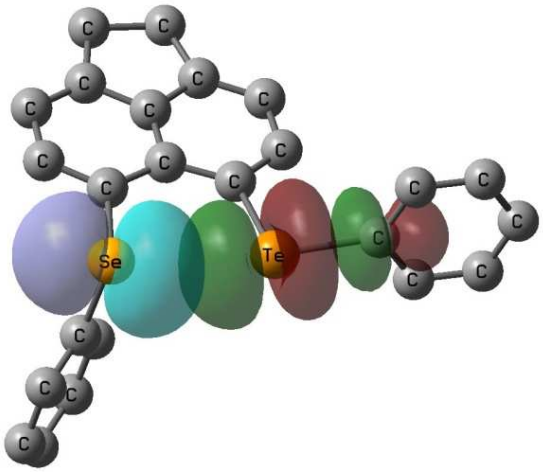


**Fig. 9** Localised natural bond orbitals in **1** BA (B3LYP level): The lone pair on one Se can act as a weak donor into the σ*(Te-$C_Y$) orbital on the other side of the *peri*-gap. Hydrogen atoms omitted for clarity.

of **1-9** (*J*(Te,Se) within 67 Hz), the extent of covalent bonding between Te and Se is predicted to be consistent throughout the series. Indeed, similar WBIs[22] are obtained in the region of 0.1 units, although this value is slightly lower than found in bis-tellurium species Acenap$(TePh)_2$ (0.14),[17] indicating a reduction in multicenter bonding in the mixed systems. Nevertheless, a significant donor-acceptor interaction is encountered in the second-order perturbation analysis of the natural bond orbitals (NBOs),[31] involving a p-type lone pair on Se and a σ*(Te-$C_Y$) antibonding orbital. The primary NBOs are plotted for **1** (TePh) in Figure 9, where this donor-acceptor interaction is predicted to be worth *ca*. 42-45 kJ $mol^{-1}$, again slightly smaller than in the ditelluride, where this interaction amounts to *ca*. 50 kJ $mol^{-1}$.

## Experimental section

All experiments were carried out under an oxygen- and moisture-free nitrogen atmosphere using standard Schlenk techniques and glassware. Reagents were obtained from commercial sources and used as received. Dry solvents were collected from a MBraun solvent system. Elemental analyses were performed by Stephen Boyer at the London Metropolitan University. Infra-red spectra were recorded for solids as KBr discs and oils on NaCl plates in the range 4000-300 $cm^{-1}$ on a Perkin-Elmer System 2000 Fourier transform spectrometer. $^1$H and $^{13}$C NMR spectra were recorded on a Bruker Avance 300 MHz spectrometer with δ(H) and δ(C) referenced to external $Me_4Si$. $^{77}$Se and $^{125}$Te NMR spectra were recorded on a Jeol GSX 270 MHz spectrometer with δ(Se) and δ(Te) referenced to external $Me_2Se$ and $Me_2Te$ respectively, with a secondary reference for δ(Te) to diphenyl ditelluride (δ(Te) = 428 ppm). Assignments of $^{13}$C and $^1$H NMR spectra were made with the help of H-H COSY and HSQC experiments. All measurements were performed at 25 °C. All values reported for NMR spectroscopy are in parts per million (ppm). Coupling constants (*J*) are given in Hertz (Hz). Electrospray Mass Spectrometry (ESMS) was performed by the University of St. Andrews Mass Spectrometry service on a Micromass LCT orthogonal accelerator time of flight mass spectrometer. Acenaphthene precursor 5-bromo-6(phenylselenyl)acenaphthene was prepared following standard literature procedures.[17] Bis(4-fluorophenyl) ditelluride (FpTeTeFp), bis(4-methylphenyl) ditelluride (TolTeTeTol), bis(4-methoxyphenyl) ditelluride (An-*p*TeTeAn-*p*), bis(2-methoxyphenyl) ditelluride (An-*o*TeTeAn-*o*), bis(4-*tert*butylphenyl) ditelluride (TpTeTeTp), bis(2,4,6-trimethylphenyl) ditelluride (MesTeTeMes), bis(2,4,6-triisopropanylphenyl) ditelluride (TipTeTeTip) and bis(1-naphthyl) ditelluride (NapTeTeNap) were synthesised from the respective aryl bromides following the procedure outlined by Ando and co-workers.[32]

**5-(4-fluorophenyltelluro)-6-(phenylselenyl)acenaphthene [Acenap(TeFp)(SePh)] (2):** To a solution of 5-bromo-6-(phenylselenyl)acenaphthene [Acenap(Br)(SePh)] (0.87 g, 2.25 mmol) in diethyl ether (40 mL) at -78 °C was added dropwise a 2.5 M solution of *n*-butyllithium in hexane (0.9 mL, 2.25 mmol). The mixture was stirred at this temperature for 1 h after which a solution of bis(4-flurorophenyl) ditelluride [$(FpTe)_2$] (1.00 g, 2.25 mmol) in diethyl ether (80 mL) was added dropwise to the mixture. The resulting mixture was stirred at -78 °C for a further 1 h and then allowed to warm to room temperature. The reaction mixture was then washed with 0.1 M aqueous sodium hydroxide

Cite this: DOI: 10.1039/c0xx00000x

www.rsc.org/xxxxxx

# ARTICLE TYPE

**Table 4** Selected interatomic distances [Å] and angles [°] for compounds **2-5**

| **Compound** | **2** | **3** | **4** | **5** |
|---|---|---|---|---|
| *Peri*-atoms | TeFp, SePh | TeTol, SePh | TeAn-*p*, SePh | TeAn-*o*, SePh |
| ***Peri-region-distances*** | | | | |
| Te(1)···Se(1) | 3.2177(7) | 3.2289(8) [3.2021(8)] | 3.2132(15) | 3.2127(17) [3.2792(18)] |
| $\%\Sigma r_{vdW}$[a] | 81 | 82 [81] | 81 | 81 [83] |
| ***Acenaphthene bond lengths*** | | | | |
| C(1)-C(2) | 1.388(4) | 1.375(7) [1.389(7)] | 1.360(15) | 1.370(10) [1.390(13)] |
| C(2)-C(3) | 1.395(5) | 1.406(5) [1.406(5)] | 1.394(15) | 1.420(13) [1.430(14)] |
| C(3)-C(4) | 1.370(5) | 1.355(8) [1.352(7)] | 1.368(14) | 1.364(15) [1.362(15)] |
| C(4)-C(5) | 1.414(4) | 1.413(7) [1.417(7)] | 1.407(17) | 1.397(11) [1.371(12)] |
| C(5)-C(10) | 1.413(5) | 1.413(5) [1.410(5)] | 1.411(16) | 1.442(14) [1.436(12)] |
| C(5)-C(6) | 1.404(4) | 1.400(7) [1.398(7)] | 1.408(15) | 1.416(15) [1.416(16)] |
| C(6)-C(7) | 1.366(4) | 1.372(8) [1.366(8)] | 1.36(2) | 1.398(11) [1.373(15)] |
| C(7)-C(8) | 1.407(5) | 1.410(5) [1.415(5)] | 1.38(3) | 1.389(15) [1.394(14)] |
| C(8)-C(9) | 1.378(5) | 1.369(7) [1.377(7)] | 1.379(17) | 1.360(16) [1.363(16)] |
| C(9)-C(10) | 1.432(4) | 1.443(7) [1.433(7)] | 1.442(16) | 1.426(11) [1.428(13)] |
| C(10)-C(1) | 1.430(4) | 1.431(7) [1.432(7)] | 1.447(13) | 1.454(14) [1.442(15)] |
| C(4)-C(11) | 1.502(5) | 1.516(5) [1.511(5)] | 1.507(16) | 1.532(15) [1.522(15)] |
| C(11)-C(12) | 1.556(4) | 1.551(8) [1.550(8)] | 1.520(18) | 1.555(14) [1.542(16)] |
| C(12)-C(6) | 1.512(5) | 1.518(5) [1.520(5)] | 1.51(2) | 1.490(13) [1.528(13)] |
| ***Peri-region bond angles*** | | | | |
| Te(1)-C(1)-C(10) | 123.24(19) | 124.1(3) [124.7(3)] | 122.6(8) | 123.5(5) [123.2(6)] |
| C(1)-C(10)-C(9) | 130.1(3) | 130.7(3) [129.2(3)] | 130.3(10) | 131.1(9) [132.0(8)] |
| Se(1)-C(9)-C(10) | 122.1(3) | 121.5(3) [122.0(3)] | 123.3(8) | 121.6(8) [121.1(7)] |
| Σ of bay angles | 375.44(19) | 376.3(5) [375.9(5)] | 376.3(15) | 376.2(13) [375.4(12)] |
| Splay angle[b] | 15.4 | 16.3 [15.9] | 16.3 | 16.2 [15.4] |
| ***Out-of-plane displacement*** | | | | |
| Te(1) | 0.360(1) | 0.365(1) [-0.285(1)] | -0.129(1) | 0.200(1) [0.305(1)] |
| Se(1) | -0.356(1) | -0.086(1) [0.263(1) | 0.100(1) | -0.071(1) [-0.395(1)] |
| ***Central naphthalene ring torsion angles*** | | | | |
| C:(6)-(5)-(10)-(1) | 177.2(2) | 179.2(4) [-178.1(4)] | -178.4(9) | 178.0(8) [176.1(7)] |
| C:(4)-(5)-(10)-(9) | 175.7(2) | 176.8(4) [-176.8(4)] | -179.9(8) | 178.4(8) [176.2(8)] |

[a] van der Waals radii used for calculations: $r_{vdW}$(Se) 1.90 Å, $r_{vdW}$(Te) 2.06 Å;[30] [b] Splay angle: Σ of the three bay region angles – 360.

(3 x 100 mL), the organic layer dried with magnesium sulfate and concentrated under reduced pressure. The residual red/orange solid was triturated with hexane to afford the purified target compound as a pale yellow solid. An analytically pure sample was obtained from recrystallisation by diffusion of hexane into a saturated solution of the compound in dichloromethane (0.51 g, 43%); mp 126-128 °C; elemental analysis (Found: C, 54.3; H, 3.2. Calc. for $C_{24}H_{17}FSeTe$: C, 54.3; H, 3.2%); $^1$H NMR (300 MHz, $CDCl_3$, 25 °C, $Me_4Si$) $\delta$ = 7.85 (1 H, d, $^3J_{HH}$ 7.2, Acenap 4-H), 7.75 (2 H, dd, $^3J_{HH}$ 8.7, $^3J_{HF}$ 6.0, Te*Fp* 12,16-H), 7.17-7.10 (4 H, m, Acenap 3,7-H, Se*Ph* 18,22-H), 7.08-7.03 (3 H, m, Se*Ph* 19,20,21-H), 6.92-6.84 (3 H, m, Acenap 8-H, Te*Fp* 13,15-H), 3.29-3.21 (4 H, m, 2 x C$H_2$); $^{19}$F{$^1$H} NMR (282 MHz, $CDCl_3$, 25 °C, $CFCl_3$) $\delta$ = -112.7(s); $^{77}$Se NMR (51.5 MHz, $CDCl_3$, 25 °C, PhSeSePh): $\delta$ = 340 (s, $J_{SeTe}$ 726); $^{125}$Te NMR (85.2 MHz, $CDCl_3$, 25 °C, PhTeTePh): $\delta$ = 653 (s, $J_{TeSe}$ 726); MS (ES$^+$): *m/z* 548.95 (100%, M + OH), 562.97 (73, M + OMe).

**5-(4-methylphenyltelluro)-6-(phenylselenyl)acenaphthene [Acenap(TeTol)(SePh)] (3):** Experimental as for compound **2** but with [Acenap(Br)(SePh)] (0.80 g, 2.06 mmol), 2.5 M *n*-butyllithium (0.9 mL, 2.25 mmol) and bis(4-methylphenyl) ditelluride [$(TolTe)_2$] (0.87 g, 1.99 mmol) to afford the target compound as a pale yellow solid. An analytically pure sample was obtained from recrystallisation by diffusion of hexane into a saturated solution of the compound in dichloromethane (0.46 g,

Cite this: DOI: 10.1039/c0xx00000x

www.rsc.org/xxxxxx

# ARTICLE TYPE

**Table 5** Selected interatomic distances [Å] and angles [°] for compounds **6-9**.

| **Compound** | **6** | **7** | **8** | **9** |
|---|---|---|---|---|
| *Peri*-atoms | TeTp, SePh | TeMes, SePh | TeTip, SePh | TeNap, SePh |
| ***Peri-region-distances*** | | | | |
| Te(1)···Se(1) | 3.2330(6) | 3.2809(7) | 3.2098(6) | 3.2586(7) |
| $\%\Sigma r_{vdW}$[a] | 82 | 83 | 81 | 82 |
| ***Acenaphthene bond lengths*** | | | | |
| C(1)-C(2) | 1.385(5) | 1.390(5) | 1.382(7) | 1.379(5) |
| C(2)-C(3) | 1.410(5) | 1.401(5) | 1.408(8) | 1.411(5) |
| C(3)-C(4) | 1.363(5) | 1.358(4) | 1.358(8) | 1.358(5) |
| C(4)-C(5) | 1.404(5) | 1.411(5) | 1.409(7) | 1.403(5) |
| C(5)-C(10) | 1.415(5) | 1.416(4) | 1.419(8) | 1.415(5) |
| C(5)-C(6) | 1.416(4) | 1.419(4) | 1.412(8) | 1.416(5) |
| C(6)-C(7) | 1.363(5) | 1.359(5) | 1.356(8) | 1.356(6) |
| C(7)-C(8) | 1.399(5) | 1.409(5) | 1.417(9) | 1.406(6) |
| C(8)-C(9) | 1.379(5) | 1.381(4) | 1.378(8) | 1.390(5) |
| C(9)-C(10) | 1.423(5) | 1.440(4) | 1.428(7) | 1.431(5) |
| C(10)-C(1) | 1.430(4) | 1.430(4) | 1.438(7) | 1.437(4) |
| C(4)-C(11) | 1.512(5) | 1.506(5) | 1.513(9) | 1.509(5) |
| C(11)-C(12) | 1.537(5) | 1.543(5) | 1.536(8) | 1.539(5) |
| C(12)-C(6) | 1.509(5) | 1.509(5) | 1.513(8) | 1.511(6) |
| ***Peri-region bond angles*** | | | | |
| Te(1)-C(1)-C(10) | 123.4(3) | 124.5(3) | 124.0(4) | 123.8(3) |
| C(1)-C(10)-C(9) | 130.0(3) | 130.4(3) | 130.5(5) | 130.4(3) |
| Se(1)-C(9)-C(10) | 123.1(2) | 123.8(2) | 122.3(4) | 123.5(3) |
| Σ of bay angles | 376.5(5) | 378.7(5) | 376.8(7) | 377.7(5) |
| Splay angle[b] | 16.5 | 18.7 | 16.8 | 17.7 |
| ***Out-of-plane displacement*** | | | | |
| Te(1) | 0.332(1) | -0.058(1) | -0.126(1) | -0.319(1) |
| Se(1) | -0.294(1) | -0.220(1) | 0.084(1) | 0.086(1) |
| ***Central naphthalene ring torsion angles*** | | | | |
| C:(6)-(5)-(10)-(1) | 179.2(3) | 179.7(2) | -178.9(4) | -179.0(3) |
| C:(4)-(5)-(10)-(9) | 176.7(3) | 178.7(2) | -178.0(4) | -177.5(3) |

[a] van der Waals radii used for calculations: $r_{vdW}$(Se) 1.90 Å, $r_{vdW}$(Te) 2.06 Å;[30] [b] Splay angle: Σ of the three bay region angles – 360.

42%); mp 145-147 °C; elemental analysis (Found: C, 56.9; H, 3.9. Calc. for $C_{25}H_{20}SeTe$: C, 57.0; H, 3.8%); $^1$H NMR (300 MHz, $CDCl_3$, 25 °C, $Me_4Si$) $\delta$ = 7.99 (1 H, d, $^3J_{HH}$ 8.0, Acenap 4-H), 7.84 (2 H, d, $^3J_{HH}$ 7.9, Te*Tol* 12,16-H), 7.36 (1 H, d, $^3J_{HH}$ 7.5, Acenap 7-H), 7.32-7.15 (8 H, m, Acenap 3-H, Te*Tol* 13,15-H, Se*Ph* 19,20,21,22,23-H), 7.00 (1 H, d, $^3J_{HH}$ 7.5, Acenap 8-H), 3.44-3.32 (4 H, m, 2 x $CH_2$), 2.44 (3 H, s, $CH_3$); $^{77}$Se NMR (51.5 MHz, $CDCl_3$, 25 °C, PhSeSePh): $\delta$ = 342 (s, $J_{SeTe}$ 723); $^{125}$Te NMR (85.2 MHz, $CDCl_3$, 25 °C, PhTeTePh): $\delta$ = 649 (s, $J_{TeSe}$ 723); MS ($ES^+$): *m/z* 559.09 (100%, M + OMe).

**5-(4-methoxyphenylltelluro)-6-(phenylselenyl)acenaphthene [Acenap(TeAn-*p*)(SePh)] (4):** Experimental as for compound **2** but with [Acenap(Br)(SePh)] (0.87 g, 2.25 mmol), 2.5 M *n*-butyllithium (0.9 mL, 2.25 mmol) and bis(4-methoxyphenyl) ditelluride [(Ani-*p*Te)$_2$] (1.06 g, 2.25 mmol) to afford the target compound as a cream solid. An analytically pure sample was obtained from recrystallisation by diffusion of hexane into a saturated solution of the compound in dichloromethane (0.84 g, 69%); mp 164-165 °C; elemental analysis (Found: C, 55.1; H, 3.7. Calc. for $C_{25}H_{20}OSeTe$: C, 55.3; H, 3.7%). $^1$H NMR (300 MHz, $CDCl_3$, 25 °C, $Me_4Si$) $\delta$ = 8.00 (1 H, d, $^3J_{HH}$ 7.1, Acenap 4-H), 7.87 (2 H, d, $^3J_{HH}$ 8.6, Te*An-p* 12,16-H), 7.35-7.30 (3 H, m, Acenap 7-H, Se*Ph* 19,23-H), 7.26 (1 H, d, $^3J_{HH}$ 7.1, Acenap 3-H), 7.24-7.19 (3 H, m, Se*Ph* 20,21,22-H), 7.02 (1 H, d, $^3J_{HH}$ 7.4, Acenap 8-H), 6.91 (2 H, d, $^3J_{HH}$ 8.6, Te*An*-p 13,15-H), 3.88 (3 H,

Cite this: DOI: 10.1039/c0xx00000x

www.rsc.org/xxxxxx

# ARTICLE TYPE

**Table 6** Torsion angles [°] categorizing the acenaphthene and aryl ring conformations in compounds **1-9**.

| **Compound** | ***Acenaphthene ring conformations*** | | ***Aryl ring conformations*** | |
|---|---|---|---|---|
| **Torsion angle** | **C10-C1-Te1-C$_R$** | **C10-C9-Se1-C$_{Ph}$** | **C1-Te1-C13-C14** | **C9-Se1-C19-C20** |
| **1** | $\theta_1$ -168.1(8) | $\theta_2$ 101.3(9) | $\gamma_1$ 83.6(7) | $\gamma_2$ -20.8(8) |
| | Acenap$_1$[a]: equatorial[f]: **type B** | Acenap$_2$[b]: axial[e]: **type A** | Ar$_1$[c]: axial: **pd** | Ph$_1$[d]: equatorial: **pl** |
| **2** | $\theta_1$ -166.65(18) | $\theta_2$ 82.25(17) | $\gamma_1$ -99.3(3) | $\gamma_2$ -166.11(16) |
| | Acenap$_1$: equatorial: **type B** | Acenap$_2$: axial: **type A** | Ar$_1$: axial: **pd** | Ph$_1$: equatorial: **pl** |
| **3** | $\theta_1$ 167.6(3) [-168.7(4)] | $\theta_2$ 94.4(3) [-86.6(4)] | $\gamma_1$ 95.5(3) [-114.0(3)] | $\gamma_2$ -142.2(4) [138.9(4)] |
| | Acenapyl$_1$: equatorial: **type B** | Acenap$_2$: axial: **type A** | Ar$_1$: axial: **pd** [twist: **np**] | Ph$_1$: twist: **np** [twist: **np**] |
| **4** | $\theta_1$ -174.8(6) | $\theta_2$ -99.3(8) | $\gamma_1$ 98.5(6) | $\gamma_2$ -109.3(7) |
| | Acenap$_1$: equatorial: **type B** | Acenap$_2$: axial: **type A** | Ar$_1$: axial: **pd** | Ph$_1$: axial: **pd** |
| **5** | $\theta_1$ -179.8(6) [162.4(6)] | $\theta_2$ -122.4(7) [-123.4(6)] | $\gamma_1$ 78.4(7) [90.0(6)] | $\gamma_2$ 59.9(8) [81.9(7)] |
| | Acenap$_1$: equatorial: **type B** | Acenap$_2$: twist:[g] **type C** | Ar$_1$: axial: **pd** | Ph$_1$: twist: **np** [axial: **pd**] |
| **6** | $\theta_1$ 167.3(3) | $\theta_2$ 85.9(3) | $\gamma_1$ 97.8(3) | $\gamma_2$ -178.23(19) |
| | Acenap$_1$: equatorial: **type B** | Acenap$_2$: axial: **type A** | Ar$_1$: axial: **pd** | Ph$_1$: equatorial: **pl** |
| **7** | $\theta_1$ 161.30(17) | $\theta_2$ -87.93(19) | $\gamma_1$ -70.45(18) | $\gamma_2$ -170.31(18) |
| | Acenap$_1$: equatorial: **type B** | Acenap$_2$: axial: **type A** | Ar$_1$: axial: **pd** | Ph$_1$: equatorial: **pl** |
| **8** | $\theta_1$ -177.7(3) | $\theta_2$ 99.0(3) | $\gamma_1$ 106.7(3) | $\gamma_2$ -160.8(3) |
| | Acenap$_1$: equatorial: **type B** | Acenap$_2$: axial: **type A** | Ar$_1$: axial: **pd** | Ph$_1$: equatorial: **pl** |
| **9** | $\theta_1$ -161.2(2) | $\theta_2$ 89.9(3) | $\gamma_1$ -125.8(2) | $\gamma_2$ -9.6(3) |
| | Acenap$_1$: equatorial: **type B** | Acenap$_2$: axial: **type A** | Ar$_1$: twist: **np** | Ph$_1$: equatorial: **pl** |

[a]**Acenap$_1$:** acenaphthene ring Te(1); [b]**Acenap$_2$**: acenaphthene ring Se(1); [c] **Ar$_1$**: Te(1) aryl ring; [d] **Ph$_1$**: Se(1) phenyl ring; [e] **axial**: perpendicular to C(ar)-E-C(ar) plane; [f] **equatorial**: coplanar with C(ar)-E-C(ar) plane; [g] **twist**: intermediate between axial and equatorial.

s, OC$H_3$), 3.41-3.34 (4 H, m, Acenap 9,10-H); $^{77}$Se NMR (51.5 MHz, $CDCl_3$, 25 °C, PhSeSePh): $\delta$ = 342 (s, $J_{SeTe}$ 722); $^{125}$Te NMR (85.2 MHz, $CDCl_3$, 25 °C, PhTeTePh): $\delta$ = 639 (s, $J_{TeSe}$ 722); MS (ES$^+$): *m/z* 574.99 (100%, M + OMe), 543.97 (43, M$^+$).

**5-(2-methoxyphenylltelluro)-6-(phenylselenyl)acenaphthene [Acenap(TeAn-*o*)(SePh)] (5):** Experimental as for compound **2** but with [Acenap(Br)(SePh)] (0.87 g, 2.25 mmol), 2.5 M *n*-butyllithium (0.9 mL, 2.25 mmol) and bis(2-methoxyphenyl) ditelluride [(An-*o*Te)$_2$] (1.06 g, 2.25 mmol) to afford the target compound as a light brown solid. An analytically pure sample was obtained from recrystallisation by diffusion of hexane into a saturated solution of the compound in dichloromethane (0.82 g, 67%); mp 133-137 °C; elemental analysis (Found: C, 55.3; H, 3.8. Calc. $C_{25}H_{20}OSeTe$: C, 55.3; H, 3.7%); $^1$H NMR (300 MHz, $CDCl_3$, 25 °C, $Me_4Si$) $\delta$ = 7.93 (1 H, d, $^3J_{HH}$ 7.2, Acenap 4-H), 7.83 (1 H, dd, $^3J_{HH}$ 7.4, $^4J_{HH}$ 1.6, Te*An-o* 16-H), 7.49 (1 H, d, $^3J_{HH}$ 7.4, Acenap 7-H), 7.46-7.41 (1 H, m, Te*An-o* 14-H), 7.38-7.34 (2 H, m, Se*Ph* 19,23-H), 7.25-7.19 (4 H, m, Acenap 3-H, Se*Ph* 3,20,21,22-H), 7.04 (1 H, d, $^3J_{HH}$ 7.4, Acenap 8-H), 7.00 (1 H, d, $^3J_{HH}$ 8.2, Te*An-o* 13-H), 6.94-6.89 (1 H, m, Te*An-o* 15-H), 3.83 (3 H, s, OC$H_3$), 3.38 (4 H, m, 2 x C$H_2$); $^{77}$Se NMR (51.5 MHz, $CDCl_3$, 25 °C, PhSeSePh): $\delta$ = 347 (s, $J_{SeTe}$ 748); $^{125}$Te NMR (85.2 MHz, $CDCl_3$, 25 °C, PhTeTePh): $\delta$ = 544 (s, $J_{TeSe}$ 748); MS (ES$^+$): *m/z* 574.99 (100%, M + OMe).

**5-(4-*tert*butylphenylltelluro)-6-(phenylselenyl)acenaphthene [Acenap(TeTp)(SePh)] (6):** Experimental as for compound **2** but with [Acenap(Br)(SePh)] (0.8 g, 2.06 mmol), 2.5 M *n*-butyllithium (0.9 mL, 2.25 mmol) and bis(4-*tert*butylphenyl) ditelluride [(TpTe)$_2$] (1.07 g, 2.06 mmol) to afford the target compound as a brown solid. An analytically pure sample was obtained from recrystallisation by diffusion of hexane into a saturated solution of the compound in dichloromethane (0.27 g, 23%); mp 149-141 °C; elemental analysis (Found: C, 59.0; H, 4.5. Calc. for $C_{28}H_{26}SeTe$: C, 59.1; H, 4.6%); $^1$H NMR (300 MHz, $CDCl_3$, 25 °C, $Me_4Si$) $\delta$ = 7.99 (1 H, d, $^3J_{HH}$ 7.2, Acenap 4-H), 7.87 (2 H, d, $^3J_{HH}$ 8.3, Te*Tp* 12,16-H), 7.41 (1 H, d, $^3J_{HH}$ 7.5, Acenap 7-H), 7.38 (2 H, d, $^3J_{HH}$ 8.3, Te*Tp* 13,15-H), 7.32-7.29 (2 H, m, Se*Ph* 21,25-H), 7.26 (1 H, d, $^3J_{HH}$ 7.3, Acenap 3-H), 7.23-7.17 (3 H, m, Se*Ph* 22,23,24-H), 7.03 (1 H, d, $^3J_{HH}$ 7.4, Acenap 8-H), 3.44-3.34 (4 H, m, 2 x C$H_2$), 1.40 (9 H, s, 3 x C$H_3$); $^{77}$Se NMR (51.5 MHz, $CDCl_3$, 25 °C, PhSeSePh): $\delta$ = 343 (s, $J_{SeTe}$ 723); $^{125}$Te NMR (85.2 MHz, $CDCl_3$, 25 °C, PhTeTePh): $\delta$ = 643 (s, $J_{TeSe}$ 723); MS (ES$^+$): *m/z* 601.04 (100%, M + OMe).

**5-(2,4,6-trimethylphenylltelluro)-6-(phenylselenyl)acenaphthene [Acenap(TeMes)(SePh)] (7):** Experimental as for compound **2** but with [Acenap(Br)(SePh)] (1.0 g, 2.63 mmol), 2.5 M *n*-butyllithium (1.1 mL, 2.65 mmol) and bis(2,4,6-trimethylphenyl) ditelluride [(MesTe)$_2$] (1.31 g, 2.63 mmol) to afford the target compound as a cream solid. An

analytically pure sample was obtained from recrystallisation by diffusion of hexane into a saturated solution of the compound in dichloromethane (0.30 g, 21%); mp 145-147 °C; elemental analysis (Found: C, 58.55; H, 4.3. Calc. for $C_{27}H_{24}SeTe$: C, 58.4; H, 4.4%); $^1$H NMR (300 MHz, $CDCl_3$, 25 °C, $Me_4Si$) $\delta$ = 7.89 (1 H, d, $^3J_{HH}$ 7.1, Acenap 4-H), 7.23-7.20 (2 H, m, Se*Ph* 21,25-H), 7.14 (1 H, d, $^3J_{HH}$ 7.1, Acenap 3-H), 7.12-7.06 (3 H, m, Se*Ph* 22,23,24-H), 7.04 (1 H, d, $^3J_{HH}$ 7.4, Acenap 7-H), 6.94 (2 H, s, Te*Mes* 13,15-H), 6.85 (1 H, d, $^3J_{HH}$ 7.4, Acenap 8-H), 3.30-3.23 (4 H, m, 2 x C$H_2$), 2.42 (6 H, s, Te*Mes* 17,19-H), 2.25 (3 H, s, Te*Mes* 18-H); $^{77}$Se NMR (51.5 MHz, $CDCl_3$, 25 °C, PhSeSePh): $\delta$ = 345 (s, $J_{SeTe}$ 711); $^{125}$Te NMR (85.2 MHz, $CDCl_3$, 25 °C, PhTeTePh): $\delta$ = 428 (s, $J_{TeSe}$ 711); MS (ES$^+$): *m/z* 587.12 (100%, M + OMe).

**5-(2,4,6-triisopropylphenylltelluro)-6-(phenylselenyl)acenaphthene [Acenap(TeTip)(SePh)] (8):** Experimental as for compound **2** but with [Acenap(Br)(SePh)] (0.87 g, 2.25 mmol), 2.5 M *n*-butyllithium (0.9 mL, 2.25 mmol) and bis(2,4,6-triisopropylphenyl) ditelluride [$(TipTe)_2$] (1.49 g, 2.25 mmol) to afford the target compound as a cream solid. An analytically pure sample was obtained from recrystallisation by diffusion of hexane into a saturated solution of the compound in dichloromethane (0.80 g, 56%); mp 158-160 °C; elemental analysis (Found: C, 61.8; H, 5.8. Calc. for $C_{33}H_{36}SeTe$: C, 62.0; H, 5.7%); $^1$H NMR (300 MHz, $CDCl_3$, 25 °C, $Me_4Si$) $\delta$ = 8.05 (1 H, d, $^3J_{HH}$ 7.1, Acenap 4-H), 7.41-7.38 (2 H, m, Se*Ph* H-27,31), 7.28 (1 H, d, $^3J_{HH}$ 7.1, Acenap 3-H), 7.26-7.21 (4 H, m, Acenap 7-H, Se*Ph* 28,29,30-H), 7.20 (2 H, s, Te*Tip* 13,15-H), 7.02 (1 H, d, $^3J_{HH}$ 7.4, Acenap 8-H), 3.73 (2 H, hept, $^3J_{HH}$ 6.8, Te*Tip* 17,23-H), 3.43-3.35 (4 H, m, 2 x C$H_2$), 3.04 (1 H, hept, $^3J_{HH}$ 6.9, 20-H), 1.40 (6 H, d, $^3J_{HH}$ 6.9, Te*Tip* 2 x C$H_3$), 1.21 (12 H, d, $^3J_{HH}$ 6.8, Te*Tip* 4 x C$H_3$); $^{77}$Se NMR (51.5 MHz, $CDCl_3$, 25 °C, PhSeSePh): $\delta$ = 345 (s, $J_{SeTe}$ 688); $^{125}$Te NMR (85.2 MHz, $CDCl_3$, 25 °C, PhTeTePh): $\delta$ = 376 (s, $J_{TeSe}$ 688); MS (ES$^+$): *m/z* 671.12 (100%, M + OMe).

**5-(naphthyltelluro)-6-(phenylselenyl)acenapthene [Acenap(TeNap)(SePh)] (9):** Experimental as for compound **2** but with [Acenap(Br)(SePh)] (0.79 g, 2.03 mmol), 2.5 M *n*-butyllithium (0.81 mL, 2.03 mmol) and bis(1-naphthyl) ditelluride [$(NapTe)_2$] (1.04 g, 2.03 mmol) to afford the target compound as a light brown solid. An analytically pure sample was obtained from recrystallisation by diffusion of hexane into a saturated solution of the compound in dichloromethane (0.97 g, 86%); mp 126-128 °C; elemental analysis (Found: C, 59.5; H, 3.7. Calc. for $C_{28}H_{20}SeTe$: C, 59.7; H, 3.6%); $^1$H NMR (300 MHz, $CDCl_3$, 25 °C, $Me_4Si$) $\delta$ = 8.25 (1 H, dd, $^3J_{HH}$ 6.9, $^4J_{HH}$ 1.2, Te*Nap* 14-H), 8.16 (1 H, d, $^3J_{HH}$ 7.8, Te*Nap* 15-H), 7.91 (1 H, d, $^3J_{HH}$ 7.1, Acenap 4-H), 7.86 (1 H, d, $^3J_{HH}$ 8.2, Te*Nap* 12-H), 7.73 (1 H, d, $^3J_{HH}$ 7.5, Te*Nap* 18-H), 7.41-7.34 (1 H, m, Te*Nap* 17-H), 7.32-7.27 (2 H, m, Te*Nap* 17,13-H), 7.26-7.21 (2 H, m, Se*Ph* 20,24-H), 7.17-7.07 (3 H, m, Se*Ph* 21,22,23-H), 6.97 (1 H, d, $^3J_{HH}$ 7.4, Acenap 7-H), 6.67 (1 H, d, $^3J_{HH}$ 7.4, Acenap 8-H), 3.29-3.16 (4 H, m, Acenap 9,10-H); $^{77}$Se NMR (51.5 MHz, $CDCl_3$, 25 °C, PhSeSePh): $\delta$ = 400 (s, $J_{TeSe}$ 724); $^{125}$Te NMR (85.2 MHz, $CDCl_3$, 25 °C, PhTeTePh): $\delta$ = 552 (s, $J_{TeSe}$ 724); MS (ES$^+$): *m/z* 580.98 (100%, M + O), 595.00 (70, M + OMe).

**Solid-state NMR experimental details**

$^{77}$Se and $^{125}$Te Solid state NMR were performed using a Bruker Avance III spectrometer operating at a magnetic field strength of 9.4 T, corresponding to Larmor frequencies of 76.3 ($^{77}$Se) and 126.2 ($^{125}$Te) MHz. Experiments were carried out using conventional 4- and 1.9-mm MAS probes, with MAS rates between 5 and 40 kHz. Chemical shifts are referenced relative to $(CH_3)_2Se$ at 0 ppm using the isotropic resonance of solid $H_2SeO_3$ at 1288.1 ppm as a secondary reference, and to $(CH_3)_2Te$ at 0 ppm using the isotropic resonance of solid $Te(OH)_6$ (site 1) at 692.2 ppm as a secondary reference. Transverse magnetization was obtained by cross polarization (CP) from $^1$H using optimized contact pulse durations of 8-20 ms, and two-pulse phase modulation (TPPM) $^1$H decoupling during acquisition. Spectra were acquired with recycle intervals of between 3 and 90 s, depending on the longitudinal relaxation time of the samples. The position of the isotropic resonances within the spinning sidebands patterns were unambiguously determined by recording a second spectrum at a higher MAS rate. A more detailed description of the experimental parameters for individual materials is given in the Supporting Information.

**Crystal structure analyses**

X-ray crystal structures for **2, 4-6**, **8** and **9** were determined at −148(1) °C using a Rigaku MM007 high-brilliance RA generator (Mo Kα radiation, confocal optic) and Saturn CCD system. At least a full hemisphere of data was collected using ω scans. Intensities were corrected for Lorentz, polarization, and absorption. Data for compounds **3** and **7** were collected at −100(1) °C using a Rigaku MM007 high-brilliance RA generator (Mo Kα radiation, confocal optic) and Mercury CCD system. At least a full hemisphere of data was collected using ω scans. Data for the complexes analyzed was collected and processed using CrystalClear (Rigaku).[33] Structures were solved by direct methods[34] and expanded using Fourier techniques.[35] Non-hydrogen atoms were refined anisotropically. Hydrogen atoms were refined using the riding model. All calculations were performed using the CrystalStructure[36] crystallographic software package except for refinement, which was performed using SHELXL-97.[37] These X-ray data can be obtained free of charge via www.ccdc.cam.ac.uk/conts/retrieving.html or from the Cambridge Crystallographic Data Centre, 12 Union Road, Cambridge CB2 1EZ, UK; fax (+44) 1223-336-033; e-mail: deposit@ccdc.cam.ac.uk.

**Computational details**

Geometries were fully optimised in the gas phase at the B3LYP/SDD/6-31G(d) level (compound **1** also with the PBE0 functional, see ESI for details). Wiberg bond indices[22] were obtained in a natural bond orbital analysis[31] at the same level and NMR spin-spin coupling constants $J(^{125}Te,^{77}Se)$ were calculated at the ZORA-SO/BP86/TZ2P level using the B3LYP optimised structures (Tables 1 and 2).[27]

**Acknowledgements**

Elemental analyses were performed by Stephen Boyer at the London Metropolitan University. Mass spectrometry was performed by Caroline Horsburgh at the University of St

Andrews Mass Spectrometry Service. The author(s) would like to acknowledge the use of the EPSRC UK National Service for Computational Chemistry Software (NSCCS) at Imperial College London in carrying out this work. Calculations were performed using the EaStCHEM Research Computing Facility maintained by Dr. H. Fru□chtl and a Silicon Graphics Altix cluster at NSCCS. The work in this project was supported by the Engineering and Physical Sciences Research Council (EPSRC). M.B. wishes to thank EaStCHEM and the University of St Andrews for support.

## Conclusions

A combination of X-ray crystallography, solution and solid state NMR spectroscopy and density functional theory (DFT) calculations has been used to investigate how substituents at the phenyl ring affect the bonding interactions and hence the value of spin-spin coupling constants between formally non bonded Te and Se atoms in Acenap(TeY)(SePh) (Y = Fp **2**; Tol **3**; An-*p* **4**; An-*o* **5**; Tp **6**; Mes **7**; Tip **8**; Nap **9**).

All eight compounds, except **5**, align the Te-$C_Y$ bond along the mean acenaphthene plane and the Se-$C_{Ph}$ bond perpendicular (type BA), promoting a nonbonded Se···Te-$C_Y$ 3c-4e type interaction which stabilises the molecule (G-dependence). In **5** (Y = An-o), a minor rotation around the Se-$C_{Acenap}$ bond affords a BC type conformation in the solid, however, DFT calculations show this optimises to BA configuration, and only lies 0.6 kcal $mol^{-1}$ above the fully optimised minimum.

A significant through-space intramolecular *peri*-interaction is observed between Te and Se atoms in all compounds of the study, with substantial $J(^{125}Te,^{77}Se)$ SSCCs in the range -687 Hz to -749 Hz detected in the $^{77}Se$ and $^{125}Te$ NMR spectra. Splittings of a similar magnitude were observed in the isotropic peaks of solid-state $^{77}Se$ MAS NMR spectra, although the presence of a significant chemical shielding anisotropy prevents easy determination of the full interaction tensors.

Natural bond orbital analysis affirms the onset of 3c-4e type bonding, showing a noticeable donor-acceptor interaction between a p-type lone pair on Se and a σ*(Te-C) antibonding orbital which reinforces the Te,Se couplings. The crystallographic steric parameter (θ), which is the cone angle measured from the furthest H atoms lying on the edges of the cone to the Te atom located at its vertex, was introduced to quantify the steric bulk of the aryl groups (Y). Modification to the size and electronics of Y has no apparent influence on the conformation of the molecule, the degree of molecular distortion occurring in the acenaphthene backbone or the extent of 3c-4e interaction; *peri*-distances are within 0.08 Å and no apparent correlation is observed between θ and the $^{77}Se$ chemical shifts or *J*(Te,Se) SSCCs. Good correlation is found, however, between θ and $^{125}Te$ chemical shifts. DFT calculations performed on all members of the series confirm the comparable covalent bonding between Te and Se in the series, with WBIs of *ca*. 0.1 obtained, although this value is slightly lower than in bis-tellurium species, indicating a reduction in multicenter bonding.

## Notes and references

[a] *EaStCHEM School of Chemistry and Centre for Magnetic Resonance, University of St Andrews, St Andrews KY16 9ST (UK). Fax: (+44)1334 463808; Tel:(+44)1334 463854; E-mail:jdw3@st-andrews.ac.uk*

† Electronic Supplementary Information (ESI) available: Full experimental details, computational details, X-ray crystal structure data; tables and figures. CCDC 889480–889485. See DOI: 10.1039/b000000x/

1 W. Kemp, *NMR in Chemistry; A Multinuclear Introduction*, Macmillan Education Ltd., Hampshire, England, 1986.
2 R. V. Parish, *NMR, NQR, EPR, and Mössbauer Spectroscopy in Inorganic Chemistry*, Ed. J. Burgess; Ellis Horwood, Chichester, England, 1990.
3 L. Ernst, P. Sakhaii, *Magn. Reson. Chem*. 2000, **38**, 559.
4 L. Ernst, K. Ibrom, *Angew. Chem. Int. Ed. Engl.* 1995, **34**, 1881.
5 F. B. Mallory, C. W. Mallory, K. E. Butler, M. Beth Lewis, A. Qian Xia, E. D. Luzik, Jr., L. E. Fredenburgh, M. M. Ramanjulu, Q. N. Van, M. M. Francl, D. A. Freed, C. C. Wray, C. Hann, M. Nerz-Stormes, P. J. Carroll, L. E. Chirlian, *J. Am. Chem. Soc*. 2000, **122**, 4108.
6 J. E. Peralta, V. Barone, R. H. Contreras, D. G. Zaccari, J. P. Snyder, *J. Am. Chem. Soc*. 2001, **123**, 9162.
7 S. A. Reiter, S. D. Nogai, K. Karaghiosoff, H. Schmidbaur, *J. Am. Chem. Soc*. 2004, **126**, 15833.
8 W. Nakanishi, S. Hayashi, *Chem. Eur. J*. 2008, **14**, 5645.
9 P. Kilian, F. R. Knight. J. D. Woollins, *Chem. Eur. J*. 2011, **17**, 2302.
10 P. Kilian, A. M. Z. Slawin, J. D. Woollins, *Phosphorus Sulfur Silicon Relat. Elem*. 2004, **179**, 999.
11 R. D. Jackson, S. James, A. G. Orpen, P. G. Pringle, *J. Organomet. Chem.* 1993, **458**, C3-C4.
12 P. Kilian, D. Philp, A. M. Z. Slawin, J. D. Woollins, *Eur. J. Inorg. Chem*. 2003, 249. (b) P. Kilian, A. M. Z. Slawin, J. D. Woollins, *Chem. Eur. J*. 2003, **9**, 215. (c) P. Kilian, A. M. Z. Slawin, J. D. Woollins, *Chem. Commun*. 2003, 1174. (d) P. Kilian, H. L. Milton, A. M. Z. Slawin, J. D. Woollins, *Inorg. Chem*. 2004, **43**, 2252. (e) P. Kilian, A. M. Z. Slawin, J. D. Woollins, *Inorg. Chim. Acta* 2005, **358**, 1719. (f) P. Kilian, A. M. Z. Slawin, J. D. Woollins, *Dalton Trans*. 2006, 2175. (g) P. Kilian, A. M. Z. Slawin, J. D. Woollins, *Dalton Trans*. 2003, 3876.
13 F. R. Knight, A. L. Fuller, M. Bühl, A. M. Z. Slawin and J. D. Woollins, *Chem. Eur. J*. 2010, **16**, 7503.
14 F. R. Knight, A. L. Fuller, M. Bühl, A. M. Z. Slawin and J. D. Woollins, *Chem. Eur. J*. 2010, **16**, 7605.
15 F. R. Knight, A. L. Fuller, M. Bühl, A. M. Z. Slawin and J. D. Woollins, *Chem. Eur. J*. 2010, **16**, 7617.
16 F. R. Knight, A. L. Fuller, M. Bühl, A. M. Z. Slawin and J. D. Woollins, *Inorg. Chem*., 2010, **49**, 7577. (b) F. R. Knight, K. S. Athukorala Arachchige, R. A. M. Randall, M. Bühl, A. M. Z. Slawin, J. D. Woollins, *Dalton Trans*. 2012, **41**, 3154.
17 L. K. Aschenbach, F. R. Knight, R. A. M. Randall, D. B. Cordes, A. Baggott, M. Bühl, A. M. Z. Slawin, J. D. Woollins, *Dalton Trans*. 2012, **41**, 3141.
18 F. R. Knight, R. A. M. Randall, K. S. Athukorala Arachchige, L. Wakefield, J. M. Griffin, S. E. Ashbrook, M. Bu□hl, A. M. Z. Slawin, J. D. Woollins, *Inorg. Chem.* 2012, **51**, 11087.
19 M.-L. Lechner, K. S. Athukorala Arachchige, R. A. M. Randall, F. R. Knight, M. Bühl, A. M. Z. Slawin, J. D. Woollins, *Organometallics* 2012, **31**, 2922.
20 M. Bühl, F. R. Knight, A. Křístková, I. Malkin Ondík, O. L. Malkina, R. A. M. Randall, A. M. Z. Slawin, J. D. Woollins, *Angew. Chem*. 2013, **125**, 2555; *Angew. Chem. Int. Ed*. 2013, **52**, 2495.
21 F. R. Knight, R. A. M. Randall, T. L. Roemmele, R. T. Boeré, B. E. Bode, L. Crawford, M. Bühl, A. M. Z. Slawin, J. D. Woollins, *ChemPhyChem*, 2013, **14**, 3199.
22 K. B. Wiberg, *Tetrahedron*, 1968, **24**, 1083-1096.
23 H. Fujihara, H. Ishitani, Y. Takaguchi, N. Furukawa, *Chem. Lett*. 1995, **24**, 571.
24 The magnetic equivalence of the two Te nuclei in solution impedes direct observation of $J(^{125}Te,^{125}Te)$ couplings in $^{125}Te$ NMR spectra, however, they can be converted from experimentally obtained $J(^{123}Te,^{125}Te)$ coupling detected as satellites in the $^{123}Te$ NMR.
25 W. Nakanishi, S. Hayashi, S. Toyota, *Chem. Commun.* 1996, 371; W. Nakanishi, S. Hayashi, A. Sakaue, G. Ono, Y. Kawada, *J. Am.*

*Chem. Soc.* 1998, **120**, 3635; W. Nakanishi, S. Hayashi, S. Toyota, *J. Org. Chem.* 1998, **63**, 8790; S. Hayashi, W. Nakanishi, *J. Org. Chem.* 1999, **64**, 6688; W. Nakanishi, S. Hayashi, T. Uehara, *J. Phys. Chem.* 1999, **103**, 9906; W. Nakanishi, S. Hayashi, *Phosphorus, Sulfur, Silicon Relat. Elem.* 2002, **177**, 1833; S. Hayashi, W. Nakanishi, *J. Org. Chem.* 2002, **67**, 38; S. Hayashi, W. Nakanishi, *Bull. Chem. Soc. Jpn.* 2008, **81**, 1605; S. Hayashi, K. Yamane, W. Nakanishi**,** *Bioinorganic Chemistry and Applications* 2009, 2009, **doi:10.1155/2009/347359**; T. Nakai, M. Nishino, S. Hayashi, M. Hashimoto, W. Nakanishi, *Dalton Trans*. 2012, **41**, 7485.

26 P. Nagy, D. Szabó, I. Kapovits, Á. Kucsman, G. Argay, A. Kálmán, *J. Mol. Struct*. 2002, **606**, 61.

27 Employing the same level as in: ref 20.

28 Couplings involving different sets of nuclei are best compared in terms of reduced coupling constants K; for 1,8-$C_{10}H_6X_2$ the following *K* values are obtained at the ZSO/BP86/TZ2P level (in $10^{19}$ kg $m^{-2}$ $s^{-2}$ $A^{-2}$, **in bold**): X=F, ***K*($^{19}$F,$^{19}$F) = 3.7** (*J* = 38.9 Hz); X = $PMe_2$, ***K*($^{31}$P,$^{31}$P) = 107.8** (*J* = 213 Hz); X = SeMe, ***K*($^{77}$Se,$^{77}$Se) = 776** (CC*t* isomer, *J* = 341 Hz); X = TeMe, ***K*($^{125}$Te,$^{125}$Te) = 2220** (CC*t* isomer, J = 2691 Hz). By moving down one row in the periodic table, *K* increases significantly, for example, by a factor of three between the Se and Te congeners.

29 C. A. Tolman, *J. Am. Chem. Soc*. 1970, **92**, 2953; C. A. Tolman, *J. Am. Chem. Soc*. 1970, **92**, 2956; C. A. Tolman, *Chem. Rev*. 1977, **77**, 313.

30 A. Bondi, *J. Phys. Chem*. 1964, **68**, 441

31 A. E. Reed, F. Curtiss and L. A. F. Weinhold, *Chem. Rev.,* 1988, **88**, 899.

32 M. Oba, Y. Okada, M. Endo, K. Tanaka, K. Nishiyama, S. Shimada, W. Ando, *Inorg. Chem*. 2010, **49**, 10680.

33 CrystalClear 1.6: Rigaku Corporation, 1999. CrystalClear Software User's Guide, Molecular Structure Corporation, (c) 2000. Flugrath, J. W. P. *Acta Crystallogr., Sect. D* 1999, **D55**, 1718.

34 SIR97: A. Altomare, M. Burla, M. Camalli, G. Cascarano, C. Giacovazzo, A. Guagliardi, A. Moliterni, G. Polidori, R. Spagna, *J. Appl. Cryst*. 1999, **32**, 115.

35 DIRDIF99: P. T. Beurskens, G. Admiraal, G. Beurskens, W. P. Bosman, R. de Gelder, R. Israel, J. M. M. Smits, 1999. The DIRDIF-99 program system, Technical Report of the Crystallography Laboratory, University of Nijmegen, The Netherlands.

36 CrystalStructure 3.8.1: Crystal Structure Analysis Package, Rigaku and Rigaku/MSC (2000-2006). 9009 New Trails Dr. The Woodlands TX 77381 USA.

37 SHELX97: G. M. Sheldrick, *Acta Crystallogr., Sect. A* 2008, **64**, 112.